Supporting Information

Mitochondria-targeted two-photon fluorogenic probe for dual-imaging viscosity and H_2O_2 level in Parkinson's disease models

Hao Li,[a,†] Chenqi Xin,[a,†] Gaobin Zhang,[a] Xisi Han,[a] Wenjing Qin,[a] Cheng-wu Zhang,[a] Changmin Yu,[*a] Su Jing,[*b] Lin Li[*a] and Wei Huang[a,c]

[a]Key Laboratory of Flexible Electronics (KLOFE) & Institute of Advanced Materials (IAM), Nanjing Tech University (NanjingTech), 30 South Puzhu Road, Nanjing 211800, P. R. China.

[b]School of Chemistry and Molecular Engineering, Nanjing Tech University, Nanjing 211816, P. R. China.

[c]Shaanxi Institute of Flexible Electronics (SIFE), Northwestern Polytechnical University (NPU), 127 West Youyi Road, Xi'an 710072, P. R. China

[†]These authors contributed equally to this work.

*Email: iamlli@njtech.edu.cn; iamcmyu@njtech.edu.cn; sjing@njtech.edu.cn

General Procedures

Unless otherwise noted, all chemicals were purchased from commercial suppliers and used without further purification. All reactions were carried out under a dry nitrogen protection. Reaction progress was monitored by TLC on pre-coated silica plates and spots were visualized by UV light or iodine. Silica gel 60 (200-300 mesh, Silicycle) was used for column chromatography. N, N-Dimethylformamide (DMF) and Dichloromethane (CH_2Cl_2, DCM) were distilled over CaH_2. Petroleum ether (PE, 60-90^{o}C), DCM, Ethyl acetate (EA) and Methanol (MeOH) were used as eluents for Flash column chromatography with Merck silica gel (0.040-0.063). ^{1}H and ^{13}C NMR spectra were acquired over Bruker DRX500 spectrometer in $CDCl_3$ or DMSO-d_6 at 25 ^{o}C. Chemical shifts are reported in parts per million relative to internal standard tetramethylsilane ($Si(CH_3)_4$ = 0.00 ppm) or residual solvent peaks ($CDCl_3$ = 7.26 ppm, DMSO-d_6 = 2.50 ppm, MeOD = 3.31 ppm). ^{1}H NMR coupling constants (*J*) are reported in Hertz (Hz) and multiplicity is indicated as follows: s (singlet), d (doublet), t (triplet), m (multiplet), dd (doublet of doublet). Mass spectra were recorded on a Finnigan LCQ mass spectrometer, a Shimadzu LC-IT-TOF spectrometer. Absorption spectra and fluorescence spectra were recorded using BioTek Cytation 5 Cell Imaging Multi-Mode Reader. All the measurements were performed at room temperature. All images were acquired on Zeiss LSM880 NLO (2+1 with BIG) Confocal Microscope System equipped with objective LD C-Apochromat 63x/1.15 W Corr M27, cell incubator with temperature control resolution ±0.1^{o}C, 405 nm Diode laser, Argon ion laser (458, 488 and 514 nm), HeNe laser (543 and 594 nm), and a 633 nm laser, with 8 channels AOTF for simultaneous control of 8 laser lines. Ultrapure water was used to prepare all aqueous solutions.

Experimental Section

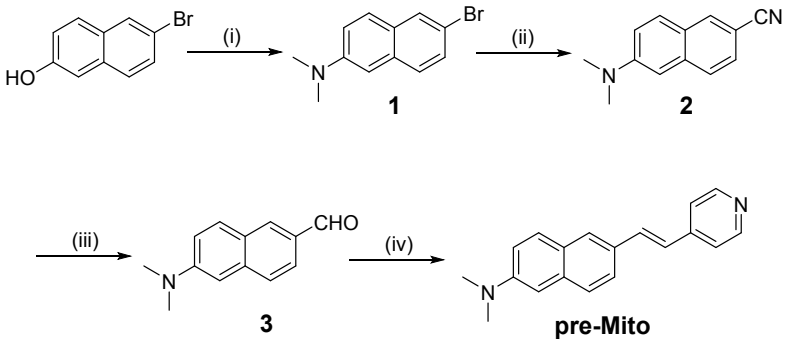

Scheme S1. Compounds 1-3 were synthesized according to reported literatures.[1, 2] Synthesized road of **pre-Mito**. Reagents and conditions. i) $Na_2S_2O_5$, Me_2NH, H_2O, 165^{o}C, 6 h, 80%; ii) CuCN, pyridine, 220^{o}C 2 h, 70%; iii) DIBAL, toluene, -78^{o}C, 30 min; room temperature, 4 h, 75%; iv) potassium *tert*-butoxide, dry DMF, 4-picline, 70%.

The response of Mito-LX to viscosity changes

The solvents were obtained by mixing methanol-glycerol systems in different proportions. Measurement was carried out with a NDJ-8S rotational viscometer, and each viscosity value was recorded. The solutions of **Mito-LX** with different viscosity were prepared by adding the stock

solution (1.0 mM) to 10 mL of solvent mixture (methanol-glycerol solvent systems) to obtain the final concentration of the **Mito-LX** (10 μM). These solutions were sonicated for 5 min to eliminate air bubbles. After standing for 1 h at a constant temperature, the solutions were measured using a microplate reader (BioTek, USA) with an excitation of 485 nm.

The effect of pH

Different values of pH (2 to 12) of PBS buffer were prepared with different concentrations of hydrochloric acid and sodium hydroxide solution with ultrapure water. The fluorescence emission spectrum at 590 nm of the probe **Mito-LX** (10 μM) with/without 10 equiv H_2O_2 were measured after incubating for 2 h in various pH solutions with an excitation of 420 nm.

Preparation of various ROS and RNS species[3]

$ONOO^-$: To a vigorously stirred solution of $NaNO_2$ (0.6 M, 10 mL) and H_2O_2 (0.7 M, 10 mL) in deionized H_2O at 0°C was added HCl (0.6 M, 10 mL), immediately followed by the rapid addition of NaOH (1.5 M, 20 mL). Excess hydrogen peroxide was removed by passing the solution through a short column of MnO_2. The concentration of $ONOO^-$ was determined by UV analysis with the extinction coefficient at 302 nm (ε = 1670 M^{-1} cm^{-1}). Aliquots of the solution were stored at -20°C for use.

NO: A solution of the H_2SO_4 (3.6 M) was added dropwise into a stirred solution of $NaNO_2$ (7.3 M). The emitted gas was allowed to pass through a solution of NaOH (2 M) first and then deionized H_2O to make a saturated NO solution of 2.0 mM.

$^1O_2$: $NaMoO_4$ (10 mM) and H_2O_2 (10 mM) were prepared in PBS (10 mM, pH 7.4). Equal aliquots of these solutions were then mixed to yield $^1O_2$ of 5 mM.

H_2O_2 and ClO^-: H_2O_2 and NaClO solution were prepared by diluting commercial H_2O_2 and NaClO solutions with PBS (10 mM, pH 7.4) to make 10 mM stock solutions.

•OH: •OH was generated by Fenton reaction. To a solution of H_2O_2 (1.0 mM, 1.0 mL) in PBS (10 mM, pH 7.4) was added $FeSO_4$ solution (1.0 mM, 100 μL) at ambient temperature (stock solution 0.1 mM).

ROO•: ROO• was generated from 2,2'-azobis(2-amidinopropane) dihydrochloride, which was dissolved in PBS (10 mM, pH 7.4) 1 h before use to make a stock solution of 10 mM.

Quantum Yield and two-photon absorption cross-section measurement

Quantum yield was determined using courmain-6 as a standard. Fluorescence quantum yield was determined by the following equation:

$$\Phi X = \frac{\Phi_{ST} * A_{ST} * F_X * \eta X^2}{A_X * F_{ST} * \eta ST^2} \qquad (1)$$

Φ is the quantum yield; A is the absorbance at the excitation wavelength (A was kept at ≤0.05 during fluorescence measurements to avoid self-quenching), F is the fluorescence intensity at the excitation

wavelength; η is the refractive index of the solvent. The subscripts ST and X refer to the standard and unknown respectively. Quantum yield of courmain-6 is 0.8 in ethanol.[4] Φ of **Mito-LX** was 0.10 and Φ of **pre-Mito** was 0.49 in PBS (contains 30% DMSO with pH = 8.0).

The two-photon cross-section (σ) and action cross-section (Φσ) was measured by using the two-photon induced fluorescence measurement technique with the following equation.

$$\sigma_S = \sigma_r \frac{F_s \Phi_r C_r \eta_r}{F_r \Phi_s C_s \eta_s} \qquad (2)$$

The subscripts "s" and "r" stand for the sample and reference molecules respectively. F is the integrated fluorescence intensities measured at the same power of the excitation beam. Φ is the fluorescence quantum yield. η is refractive index. The number density of the molecules in the solution was denoted as C. σ_r is the two-photon cross section of the reference molecule. The two-photon cross sections (Φ) of **Mito-LX** and **pre-Mito** were calculated to be 854.89 GM and 1166.99 GM, respectively.

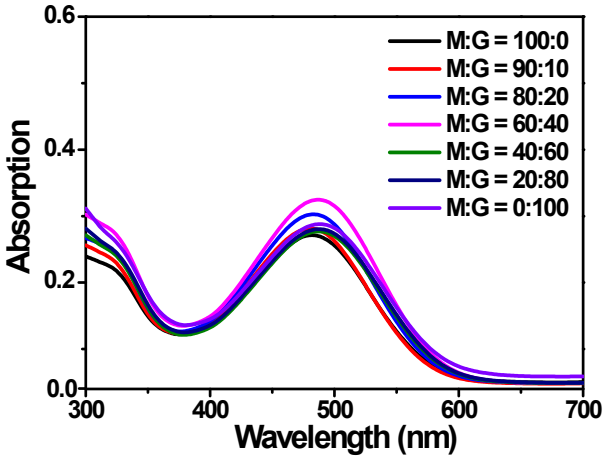

Fig. S1. UV-vis absorption of **Mito-LX** (10 μM) in the solution with different ratios of methanol (M)-glycerin (G).

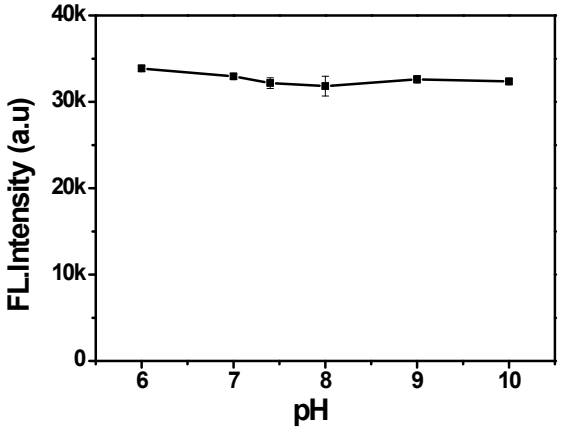

Fig. S2. Fluorescence intensity at 730 nm of **Mito-LX** (10 μM) in 90% glycerin/methanol with different pH values. λ_{ex} = 480 nm.

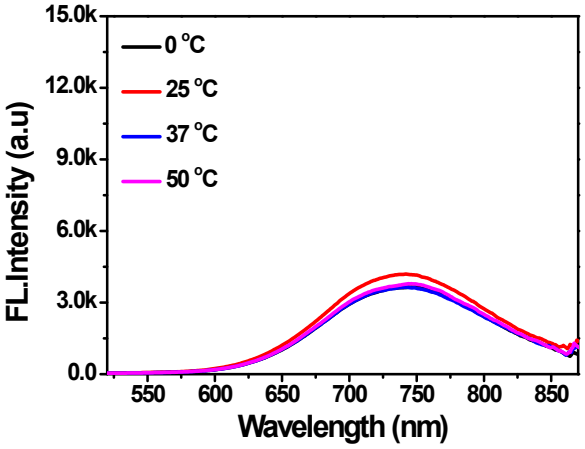

Fig. S3. Fluorescence spectra of **Mito-LX** (10 μM) in 10% glycerin/methanol with different temperatures. λ_{ex} = 480 nm.

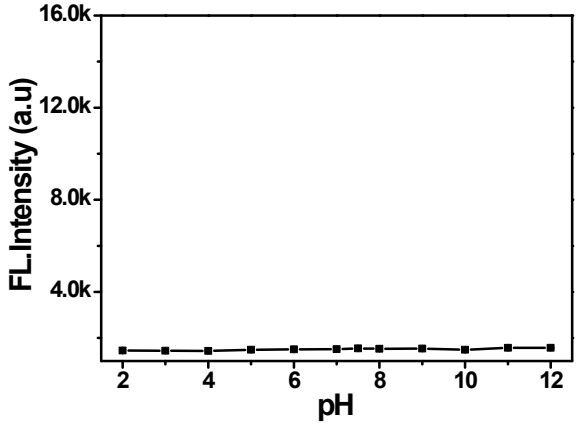

Fig. S4. Fluorescence intensity at 730 nm of **Mito-LX** (10 μM) in PBS buffer (containing 30% DMSO) with different pH values. λ_{ex} = 480 nm.

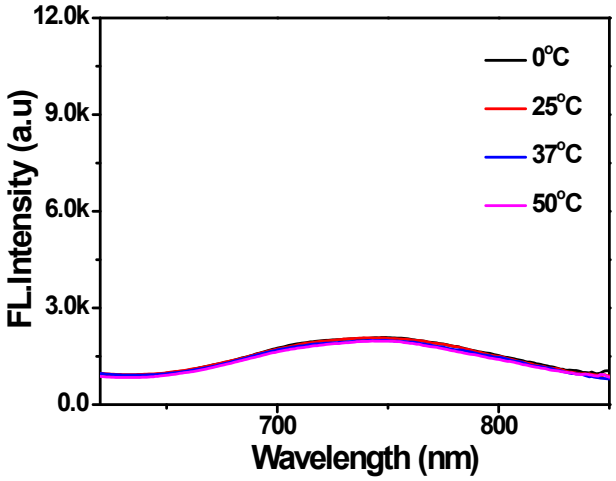

Fig. S5. Fluorescence spectra of **Mito-LX** (10 μM) in PBS buffer (containing 30% DMSO, pH = 8.0) with different temperatures. λ_{ex} = 480 nm.

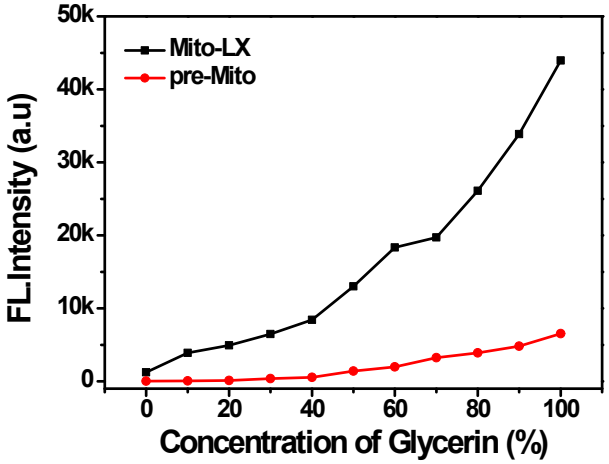

Fig. S6. Fluorescence intensity at 730 nm of **pre-Mito** (10 μM) **and Mito-LX** (10 μM) in the solution with different ratios of methanol (M)-glycerin (G), λ_{ex} = 480 nm.

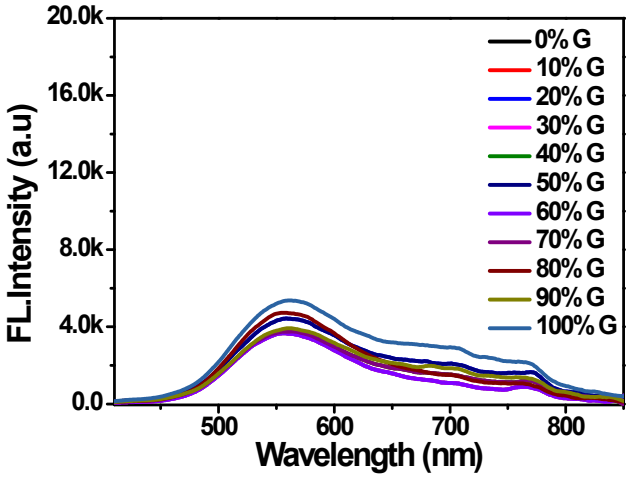

Fig. S7. Fluorescence intensity of **pre-Mito** (10 μM) in the solution with different ratios of methanol (M)-glycerin (G), λ_{ex} = 380 nm.

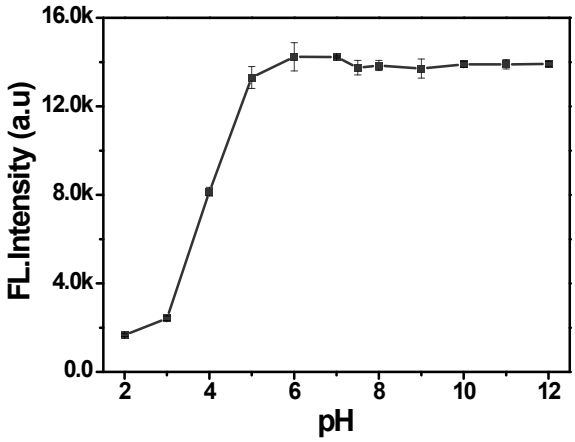

Fig. S8. Fluorescence intensity at 585 nm of **pre-Mito** (10 μM) in PBS buffer (containing 30% DMSO) with different pH values. λ_{ex} = 380 nm.

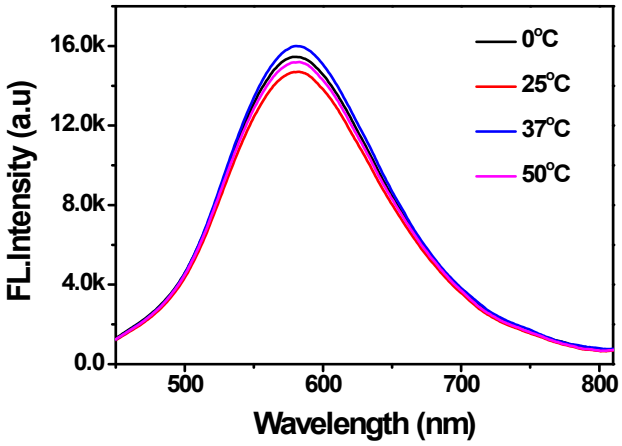

Fig. S9. Fluorescence spectra of **pre-Mito** (10 μM) in different temperature of PBS buffer (containing 30%DMSO, pH = 8.0). λ_{ex} = 420 nm.

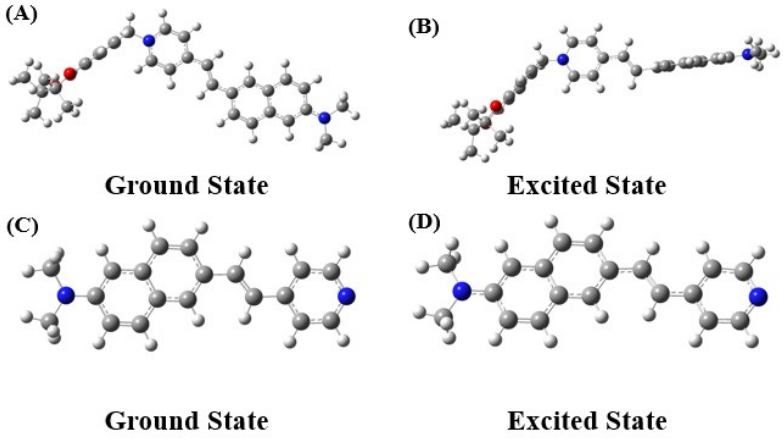

Fig. S10. DFT optimized structure of **Mito-LX** (A, B) and **pre-Mito** (C, D) in ground state and excited state. In the ball-and-stick representation, hydrogen, carbon, nitrogen, oxygen and boron atoms are colored in white, gray, blue, red and pink, respectively.

The method for determining the limit of detection (LOD)

First the calibration curve was obtained from the plot of fluorescence intensity at 585 nm, as a function of the H_2O_2 concentration. The regression curve equation was then obtained for the lower concentration part.

$$\text{The detection limit} = 3 \times \sigma / k$$

Where k is the slope of the curve equation, and σ represents the standard deviation for the probe **Mito-LX** solution's fluorescence intensity in the absence of H_2O_2. [5]

$$I_{585} = 117.49 + 3757.7[H_2O_2] \ (R = 0.9863)$$

$$\text{LOD} = 3 \times 6.2328 / 3757.7 = 4.98 \text{ nM}$$

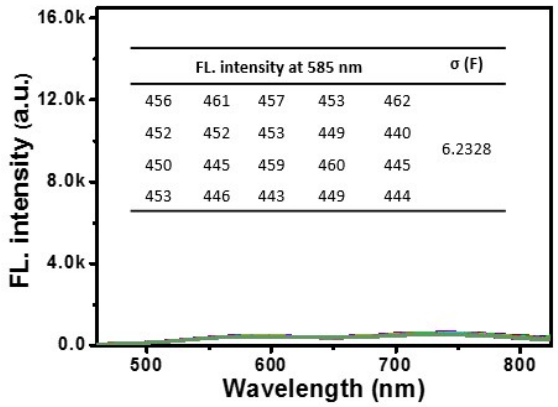

Fig. S11. Multi-recorded fluorescence spectra of blank measurement. Insert: the data of standard deviation (σ) of blank measurement from fluorescence spectra. λ_{ex} = 420 nm.

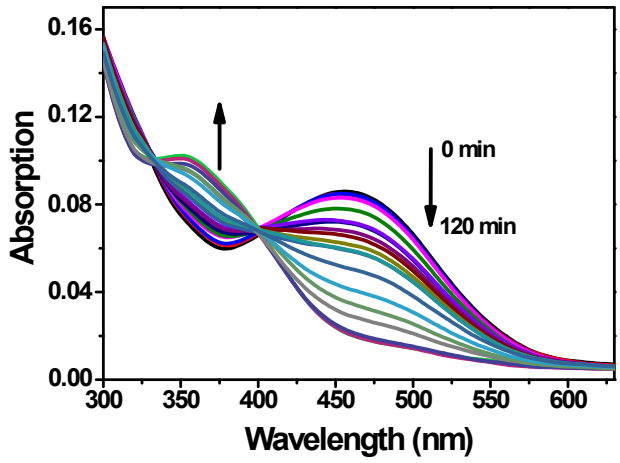

Fig. S12. UV-vis absorption of **Mito-LX** (10 μM) with H_2O_2 (100 μM) in different time in PBS buffer (containing 30%DMSO, pH = 8.0).

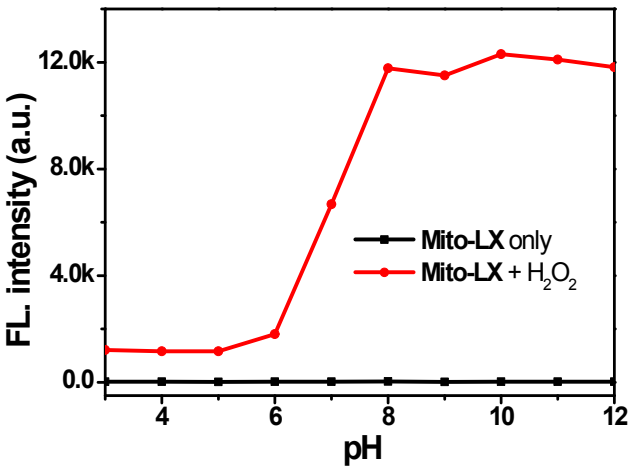

Fig. S13. Effect of pH on the fluorescence intensity at 585 nm of the **Mito-LX** (10 μM) in the absence and presence of H_2O_2. λ_{ex} = 420 nm.

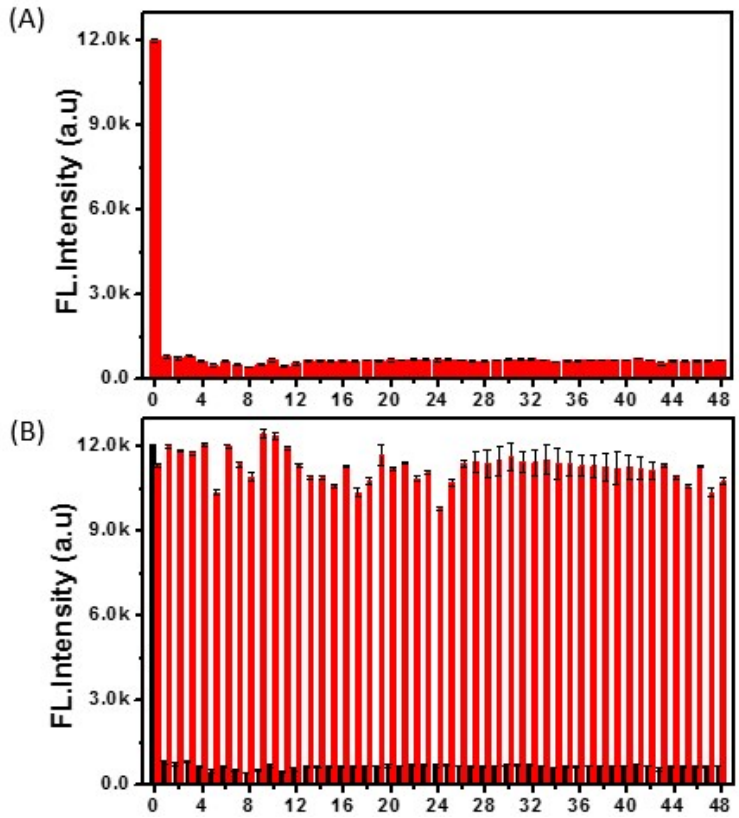

Fig. S14. (A) Fluorescence response of **Mito-LX** (10 μM) to various spices at individual concentrations of 100 μM after 2 h incubation in PBS buffer. 0. H_2O_2; 1. Na^+; 2. K^+; 3. Mg^{2+}; 4. Al^{3+}; 5. Cu^{2+}; 6. Fe^{3+}; 7. Mn^{2+}; 8. Cd^{2+}; 9. Zn^{2+}; 10. Ni^{2+}; 11. Cr^{3+}; 12. Fe^{2+}; 13. Ca^{2+}; 14. Ag^+; 15. Pd^{2+}; 16. SO_4^{2-}; 17. CH_3COO^-; 18. HCO_3^-; 19. F^-; 20. Br^-; 21. I^-; 22. NO_3^-; 23. CO_3^{2-}; 24. SO_3^{2-}; 25. HS^-; 26. SCN^-; 27. HPO_4^{2-}; 28. $H_2PO_4^-$; 29. His; 30. Val; 31. Lys; 32. Ser; 33. Ala; 34. Arg ; 35. Phe; 36. Gly; 37. Trp; 38. Thr; 39. Pro; 40. Met; 41. Cys; 42. Hcy. ; 43. $^1O_2$; 44. ^-OH; 45. ROO^-; 46. NO; 47. ClO^-. (B) Fluorescence intensities of **Mito-LX** (10 μM) treated with various species in the presence of H_2O_2 in PBS buffer. PBS buffer contains 30% DMSO with the pH = 8; $\lambda_{ex}/\lambda_{em}$ = 420/585 nm.

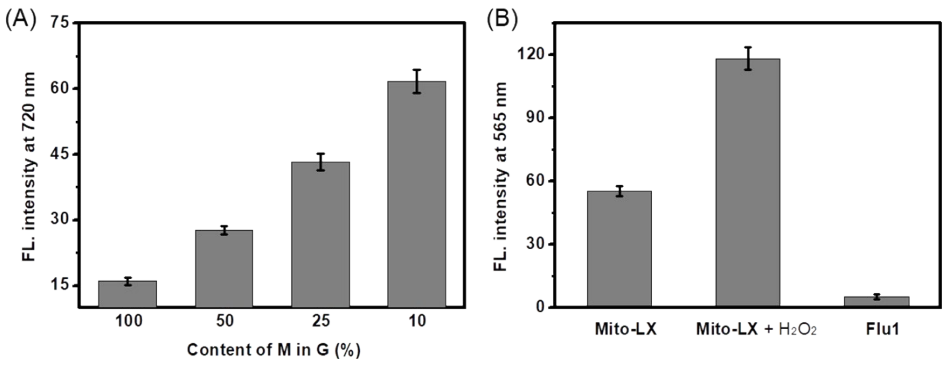

Fig. S15. (A) TP fluorescence intensity at 720 nm of **Mito-LX** (2 μM) in different ratios of methanol (M) and glycerol (G) solution. λ_{ex} = 800 nm; (B) TP fluorescence intensity at 585 nm of **Mito-LX** (2 μM) w/o H_2O_2 and the reference (**Flu1**[12], 10 μM). λ_{ex} = 760 nm.

Table S1. Properties of the representative developed fluorescent viscosity and H_2O_2 probes and the probe **Mito-LX**.

Ref.	Probe	Dual channel	λ (nm)	Detection limit (M)	Emission shift (nm)	Imaging mode	Imaging application
This work	**Mito-LX**	H_2O_2 and viscosity	420/585 485/730	4.97×10^{-9}	165/ 245	TP	HepG2 cells, zebrafishes and Drosophila brain
1[6]	**Mito-VH**	H_2O_2 and viscosity	400/510 500/607	2.1×10^{-6}	110/ 107	OP	HeLa cells
2[7]	**Lyso-HP**	H_2O_2	474/550	1.21×10^{-6}	76	TP	HeLa cells, tissue
3[8]	**TPNR-H_2O_2**	H_2O_2	560/860	7.248×10^{-8}	300	TP	MCF-7, RAW 264.7 cells,
4[9]	**Lyso-B**	viscosity	550/586	--	36	TP	HepG2 cells, HeLa cells
5[10]	**MCN**	viscosity	400/470	--	70	TP	HeLa cells, rat liver, zebrafishes
6[11]	**MHC-V1**	viscosity	470/628	--	158	OP	HeLa cells
7[11]	**MHC-V2**	viscosity	545/579	--	34	OP	HeLa cells

Noted: OP, one-photon; TP, two-photon.

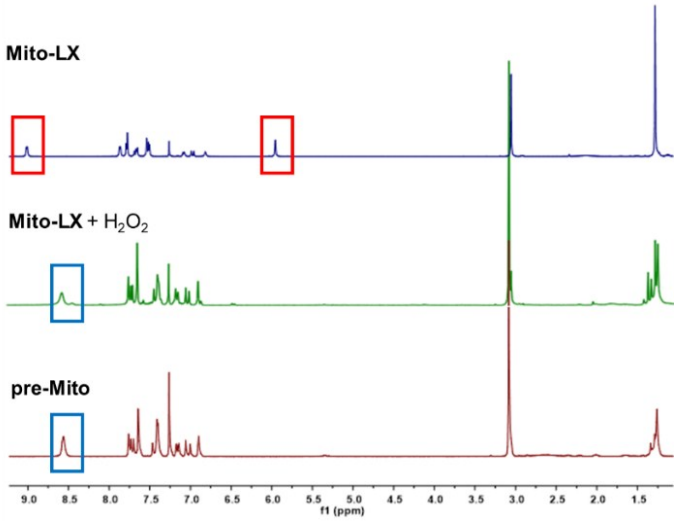

Fig. S16. The proposed mechanism of **Mito-LX** in the detection of H_2O_2. ^{1}H NMR spectra of **Mito-LX** (14 mM) obtained during the titration with H_2O_2 (140 mM) in $CDCl_3$. (Blue) ^{1}H NMR spectrum of **Mito-LX**; (Green) ^{1}H NMR spectrum of **Mito-LX** treated with H_2O_2 for 2 h and then purification; (Red) ^{1}H NMR spectrum of pure **pre-Mito**.

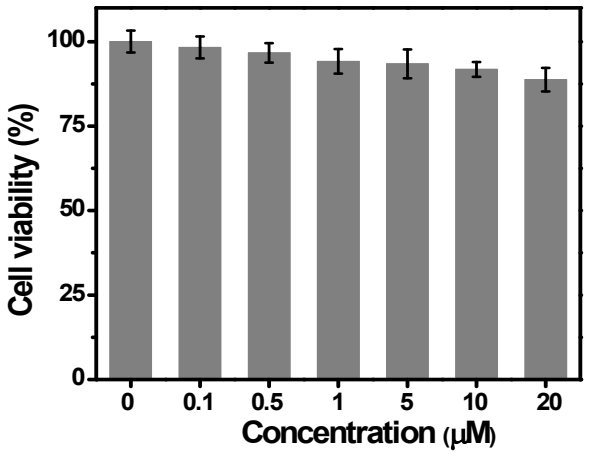

Fig. S17. Cell viability of HepG2 incubated with **Mito-LX** at different concentrations.

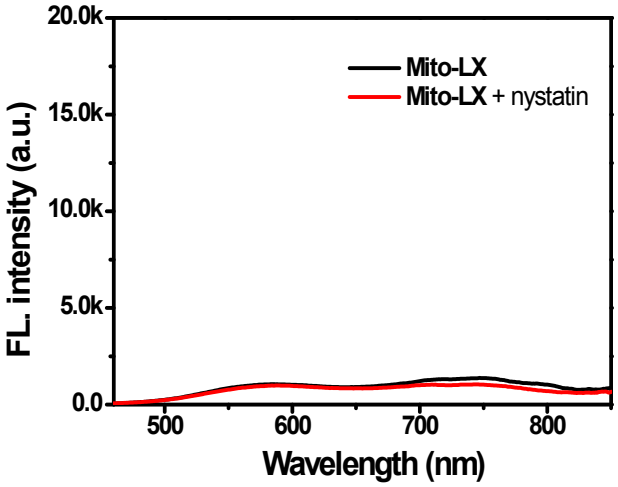

Fig. S18. Fluorescence spectra of probe **Mito-LX** (10 μM) in the absence and presence of nystatin (10 μM) in PBS buffer (pH = 8.0, containing 30% DMSO) buffer at 37°C for 30 min. λ_{ex} = 480 nm.

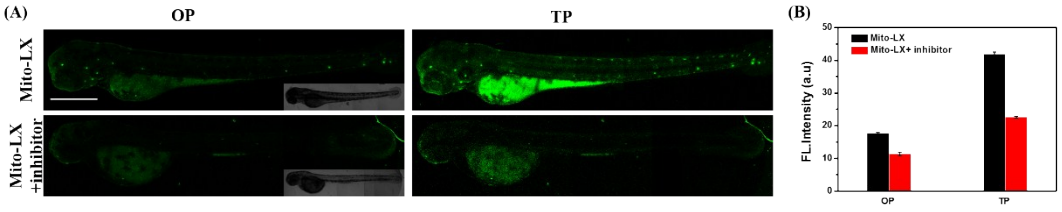

Fig. S19. (A) Confocal fluorescence images of live zebrafishes incubated with **Mito-LX** (10 μM) without/with NAC (2 μM). (B) Relative fluorescence intensity of images (A). λ_{ex} = 405 nm for OPFM, λ_{ex} = 760 nm for TPFM; PMT = 550-620 nm; Scale bar = 400 μm.

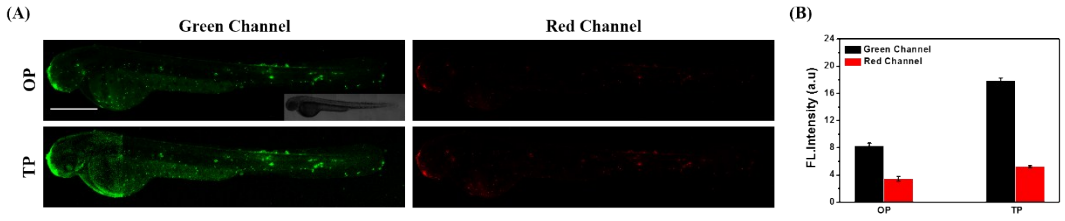

Fig. S20. (A) Confocal fluorescence images of live zebrafishes incubated with **Mito-LX** (10 μM). (B) Relative fluorescence intensity of images (A). Green channel: λ_{ex} = 405 nm for OP, λ_{ex} = 760 nm for TPFM; PMT = 550-620 nm; Red channel: λ_{ex} = 488 nm for OPFM, λ_{ex} = 800 nm for TP; PMT = 710-740 nm, Scale bar = 400 μm.

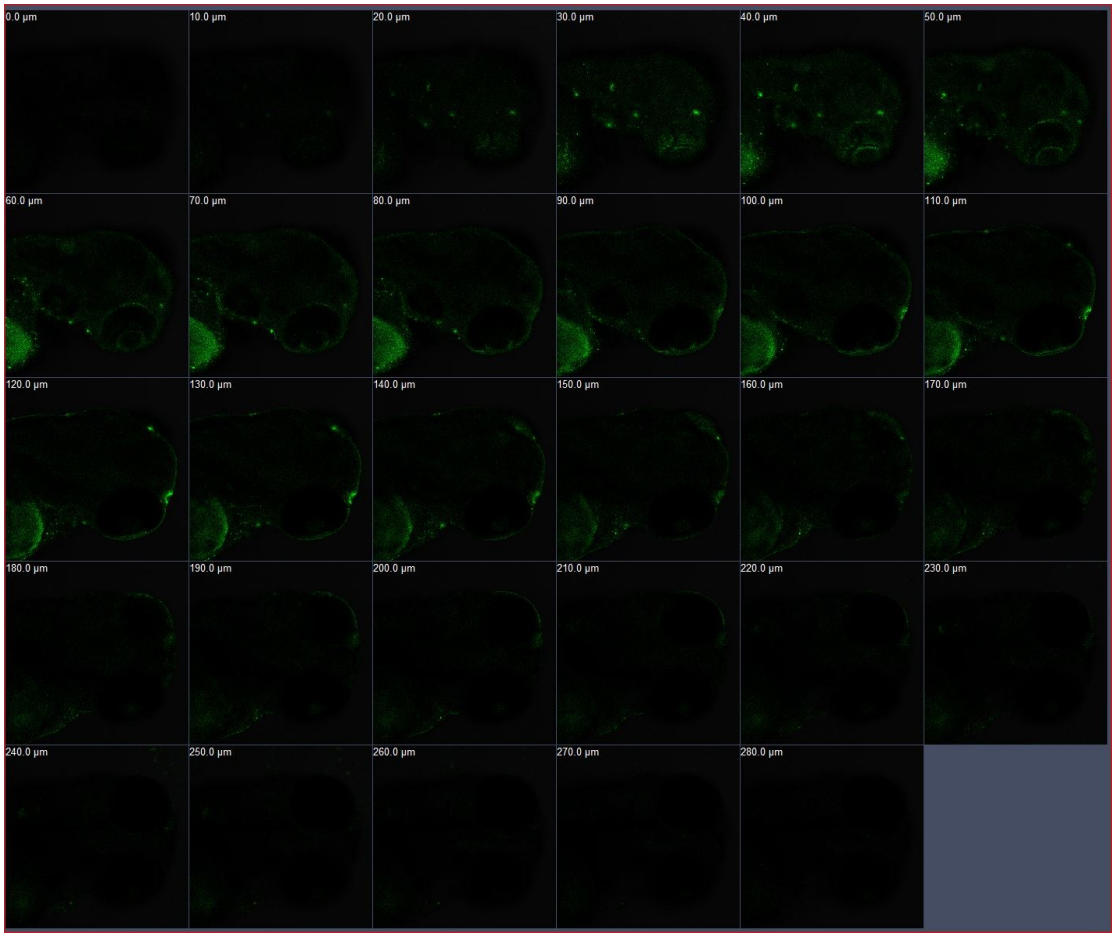

Fig. S21. *Z*-scan of two-photon fluorescence images of live zebrafish pretreated with **Mito-LX** (10 μM) incubation at depths of approximately 0 to 280 μm with a magnification of 10 μm. λ_{ex} = 800 nm for TPFM; PMT = 710-750 nm**;** Scale bar = 400 μm.

^{1}H and ^{13}C NMR spectra

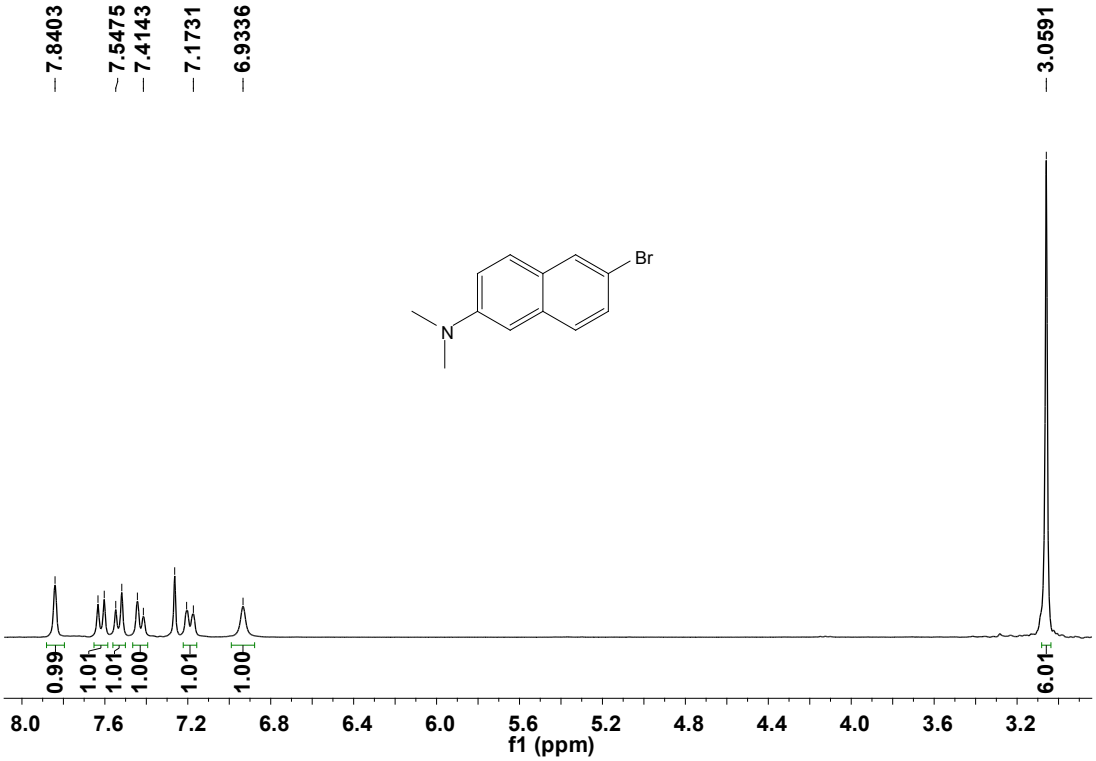

Fig. S22. ^{1}H NMR spectrum of compound **1.**

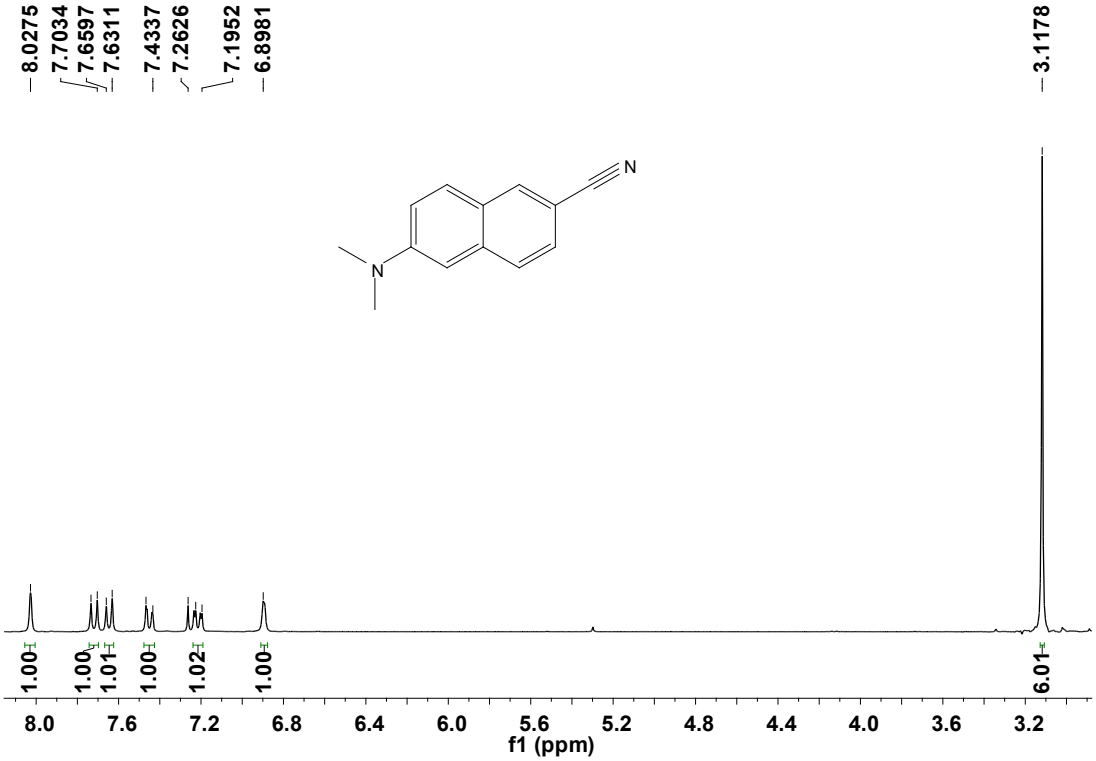

Fig. S23. ^{1}H NMR spectrum of compound **2.**

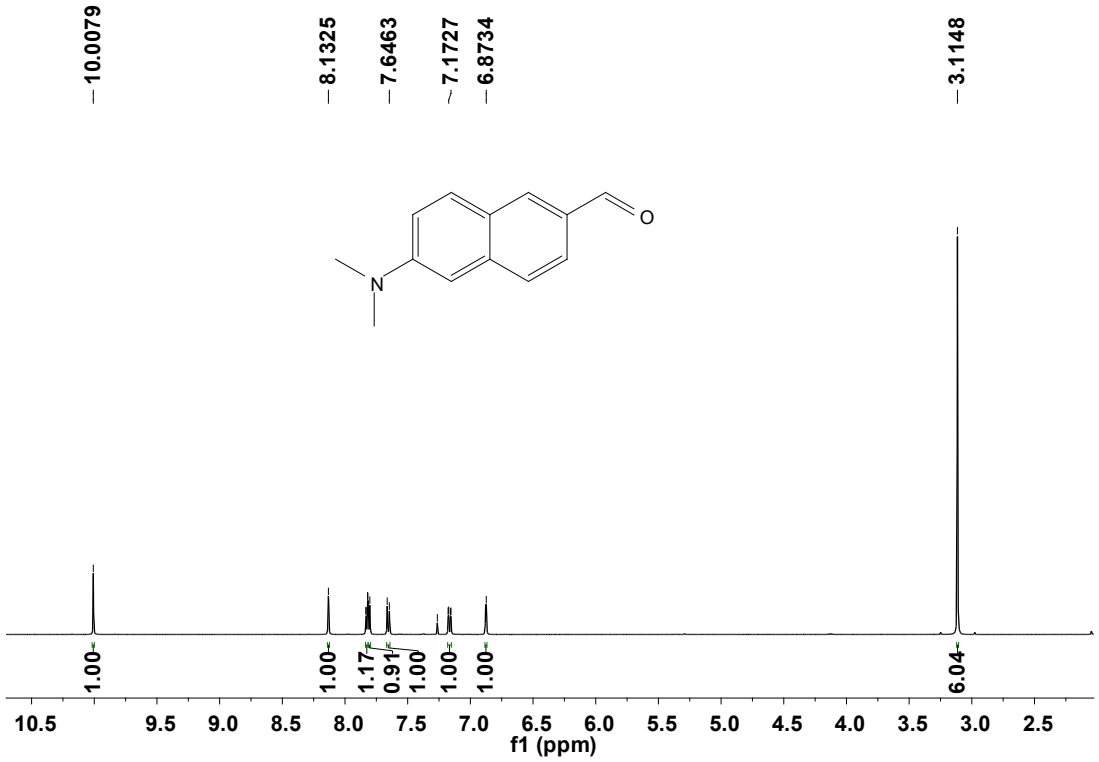

Fig. S24. [1]H NMR spectrum of compound **3.**

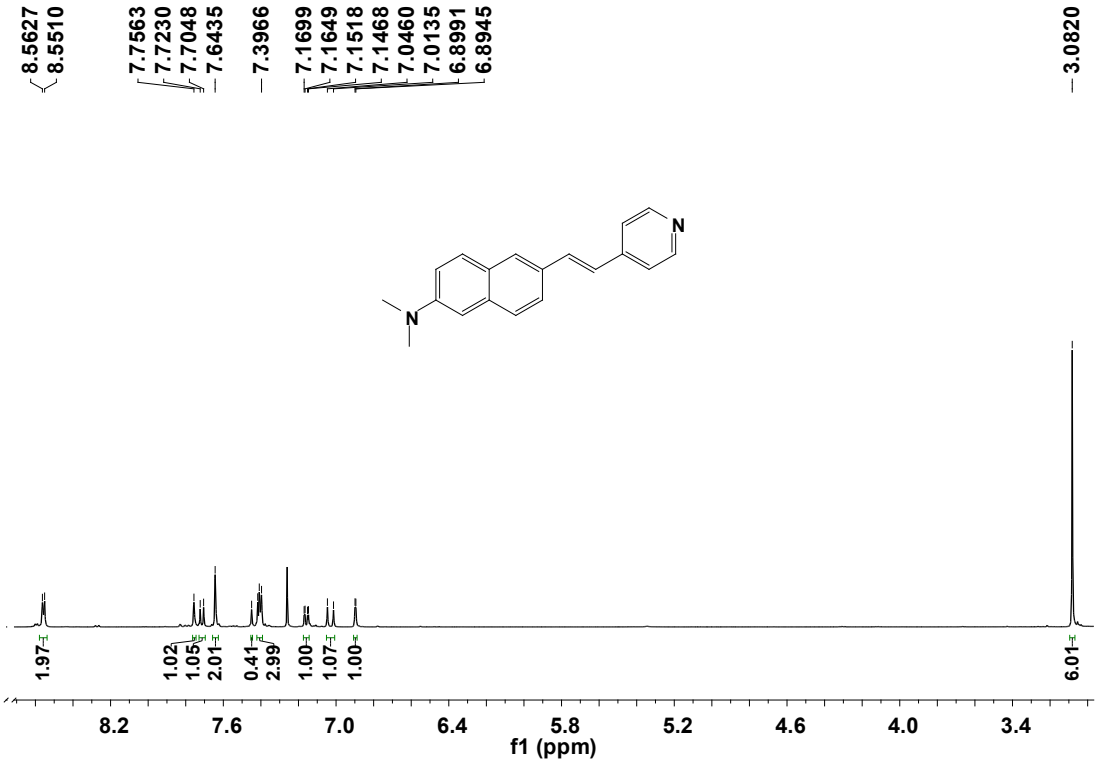

Fig. S25. [1]H NMR spectrum of **pre-Mito**.

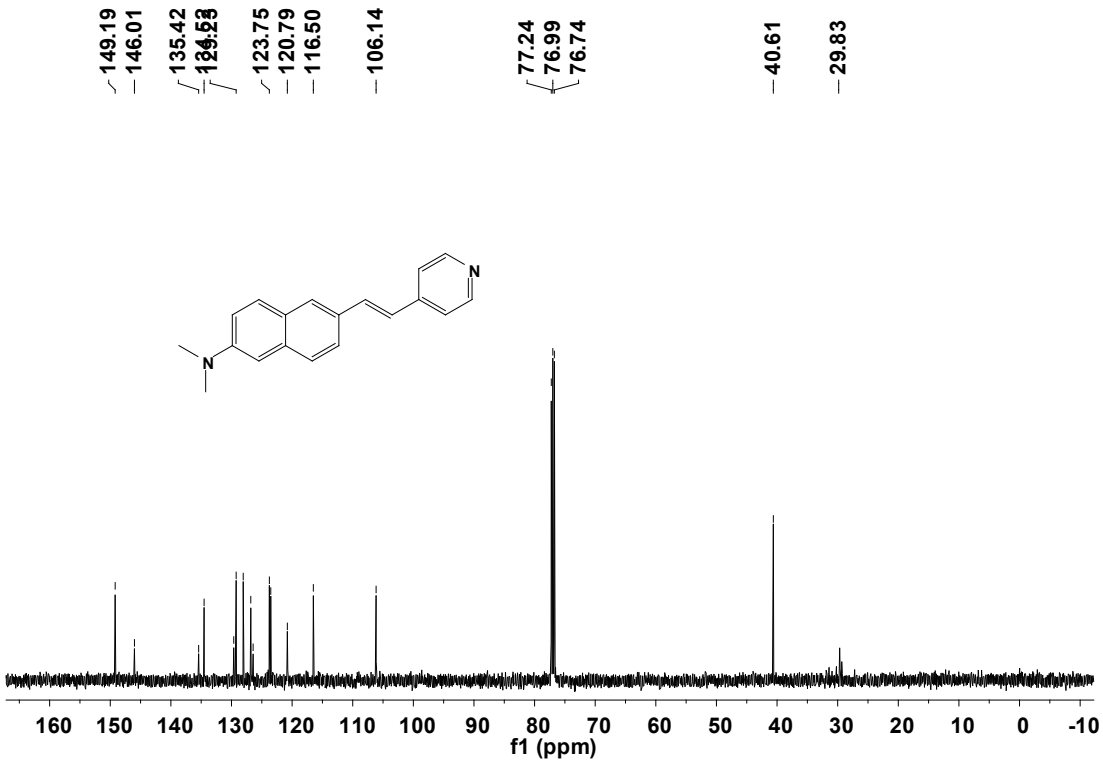

Fig. S26. ^{13}C NMR spectrum of **pre-Mito.**

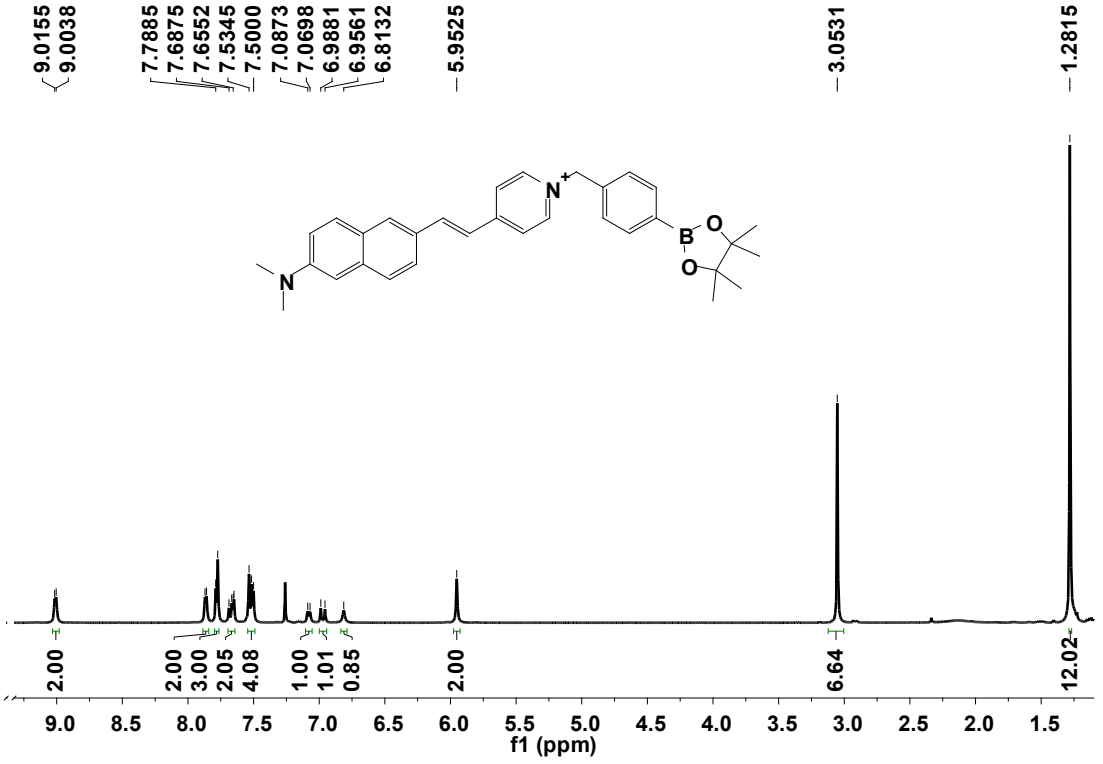

Fig. S27. ^{1}H NMR spectrum of **Mito-LX.**

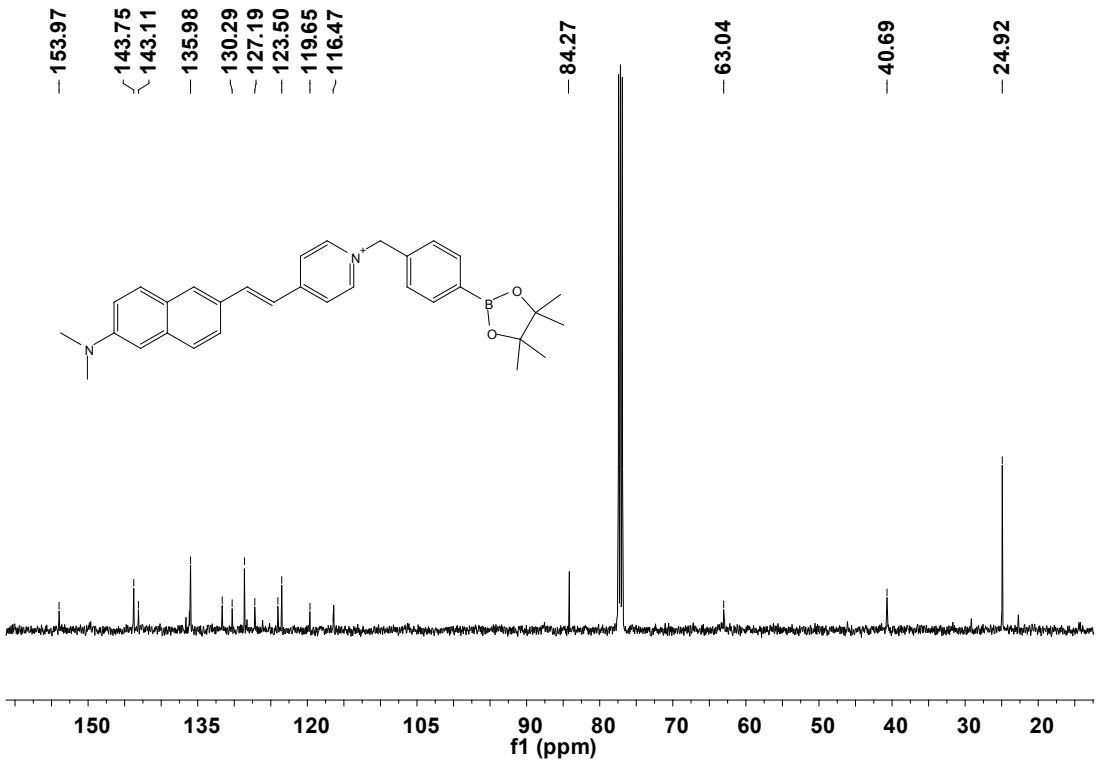

Fig. S28. ^{13}C NMR spectrum of **Mito-LX**.

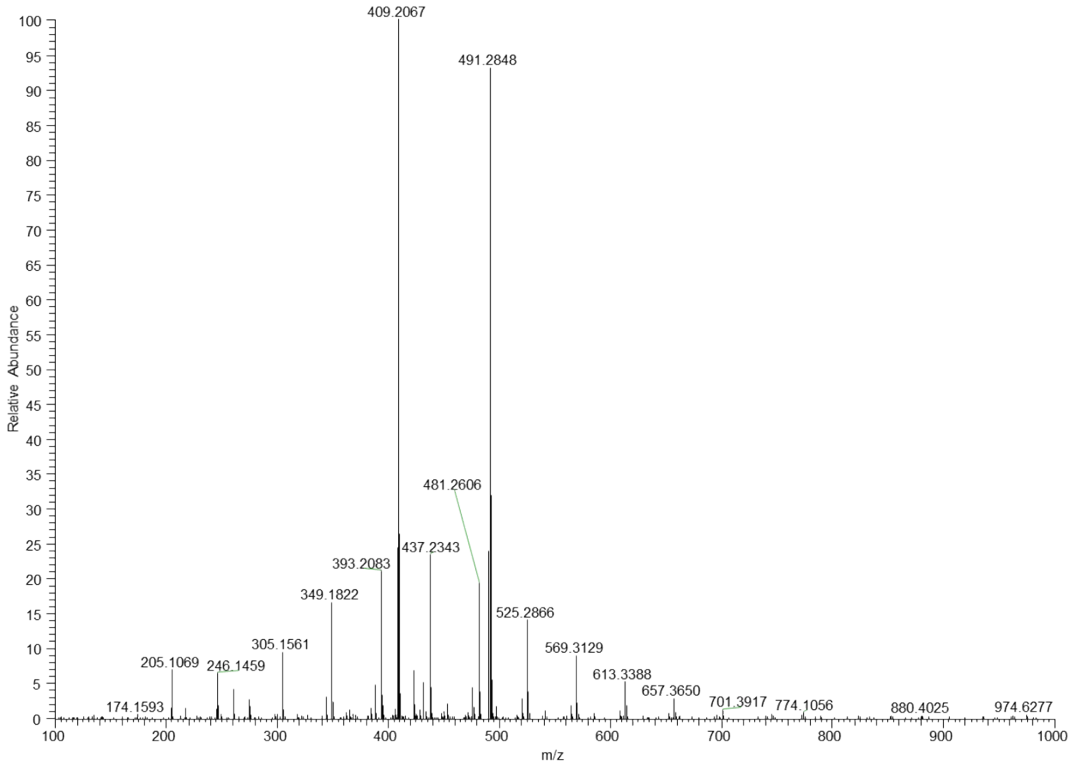

Fig. S29. HRMS of **Mito-LX**.

Reference

[1] A. S. Rao, D. Kim, T. Wang, K. H. Kim, S. Hwang, K. H. Ahn. *Org. Lett.*, 2012, **14**, 2598.

[2] L. Li, C. W. Zhang, J. Ge, L. Qian, B. H. Chai. *Angew. Chem. Int. Ed.*, 2015, **54**, 10821.

[3] X. Li, R. R. Tao, L. J. Hong, J. Cheng, Q. Jiang, Y. M. Lu, M. H. Liao, W. F. Ye, N. N. Lu, F. Han, Y. Z. Hu, Y. H. Hu. *J. Am. Chem. Soc.*, 2015, **137**, 12296.

[4] K. H. Drexhage. J. Res. *Natl. Bur. Stand.*, 1976, **80A**, 421.

[5] F. Ma, M. Liu, Z. Y. Wang and C. Y. Zhang. *Chem. Commun.*, 2016, **52**, 1218.

[6] M. Ren, B. Deng, K. Zhou, X. Kong, J. Y. Wang, W. Y. Lin. *Anal. Chem.,* 2017, **89**, 552.

[7] M. Ren, B. Deng, J. Y. Wang, X. Kong, Z. R. Liu, K. Zhou, L. He, W. Y. Lin. *Biosens. Bioelectron.,* 2016, **79**, 237.

[8] H. Li, Q. Yao, J. Fan, J. Du, J. Wang, X. Peng. *Biosens. Bioelectron.,* 2017, **94**, 536

[9] L. L. Li, K. Li, M. Y. Li, L. Shi, Y. H. Liu, H. Zhang, S. L. Pan, N. Wang, Q. Zhou, X. Q. Yu. *Anal. Chem.,* 2018, **90**, 5873.

[10] P. Ning, P. Dong, Q. Geng, L. Bai, Y. Ding, X. Tian, R. Shao, L. Li, X. Meng. *J. Mater. Chem. B.,* 2017, **15**, 2743.

[11] K. Zhou, M. Ren, B. Deng, W. Y. Lin. *New. J. Chem.,* 2017, **41**, 11507.

[12] L. Li, C. W. Zhang, G. Y. Chen, B. Zhu, C. Chai, Q. H. Xu, E. K. Tan, Q. Zhu, K. L. Lim, S. Q. Yao. *Nat. Commun.*, 2014, **5**, 3276.